National Research Institute of Astronomy and Geophysics

NRIAG Journal of Astronomy and Geophysics

www.elsevier.com/locate/nrjag

FULL LENGTH ARTICLE

Delineating active faults by using integrated geophysical data at northeastern part of Cairo, Egypt

Sultan Awad Sultan Araffa [a,*], **Fernando A. Monteiro Santos** [b],
Tarek Arafa-Hamed [a]

[a] *National Research Institute of Astronomy and Geophysics, 11722 Helwan, Egypt*
[b] *University of Lisbon, IDL, Lisbon, Portugal*

Abstract   Geophysical techniques such as gravity, magnetic and seismology are perfect tools for detecting subsurface structures of local, regional as well as of global scales. The study of the earthquake records can be used for differentiating the active and non active fault elements. In the current study more than 2200 land magnetic stations have been measured by using two proton magnetometers. The data is corrected for diurnal variations and then reduced by IGRF. The corrected data have been interpreted by different techniques after filtering the data to separate shallow sources (basaltic sheet) from the deep sources (basement complex). Both Euler deconvolution and 3-D magnetic modeling have been carried out. The results of our interpretation have indicated that the depth to the upper surface of basaltic sheet ranges from less than 10–600 m, depth to the lower surface ranges from 60 to 750 m while the thickness of the basaltic sheet varies from less than 10–450 m. Moreover, gravity measurements have been conducted at the 2200 stations using a CG-3 gravimeter. The measured values are corrected to construct a Bouguer anomaly map. The least squares technique is then applied for regional residual separation. The third order of least squares is found to be the most suitable to separate the residual anomalies from the regional one. The resultant third order residual gravity map is used to delineate the structural fault systems of different characteristic trends. The trends are a NW–SE trend parallel to that of Gulf of Suez, a NE–SW trend parallel to the Gulf of Aqaba and an E–W trend parallel to the trend of Mediterranean Sea. Taking seismological records into consideration, it is found that most of 24 earthquake events recorded in the study area are located on fault elements. This gives an indication that the delineated fault elements are active.

© 2012 National Research Institute of Astronomy and Geophysics. Production and hosting by Elsevier B.V. All rights reserved.

* Corresponding author. Mobile: +20 1222588505.
E-mail address: sultan_awad@yahoo.com (S.A. Sultan Araffa).

Production and hosting by Elsevier

Introduction

Cairo is the capital of Egypt and is the largest city in Africa and of the Arab World, being one of the most densely populated cities in the world. It consists of three governorates Cairo, Giza and Kaluobia (hence called Greater Cairo). The city is located in northern part of Egypt, known as Lower

Egypt, 165 km south of the Mediterranean Sea and 120 km west of the Gulf of Suez and Suez Canal. The city spreads on both sides of the Nile River, immediately south of the point where the river leaves its desert-bound valley and branches into the low-lying Nile Delta region. Although the metropolis Cairo extends away from the Nile in all directions, Cairo governorate resides only on the eastern bank of the river in addition to two islands within it on a total area of 214 km². Greater Cairo is affected by different fault elements (Sultan et al., 2010; Sultan and Santos, 2008; Monteiro Santos and Sultan, 2008). Sultan Awad Sultan Araffa (2010) evaluated

the structural elements in Mokattam area (east Cairo). The present study aims to detect the fault elements and their role on the distribution of the basaltic sheet; to determine the basins and uplifts as well as to estimate groundwater aquifer and oil potentiality. The last target of this study is to evaluate the active fault elements and potential effects on the environment through population and constructions.

The seismicity of Egypt is characterized by a moderate earthquake activity due to the relative motion between the African, Arabian and Eurasian plates (Abou Elenean et al., 2009). The general distribution of earthquake epicenters in
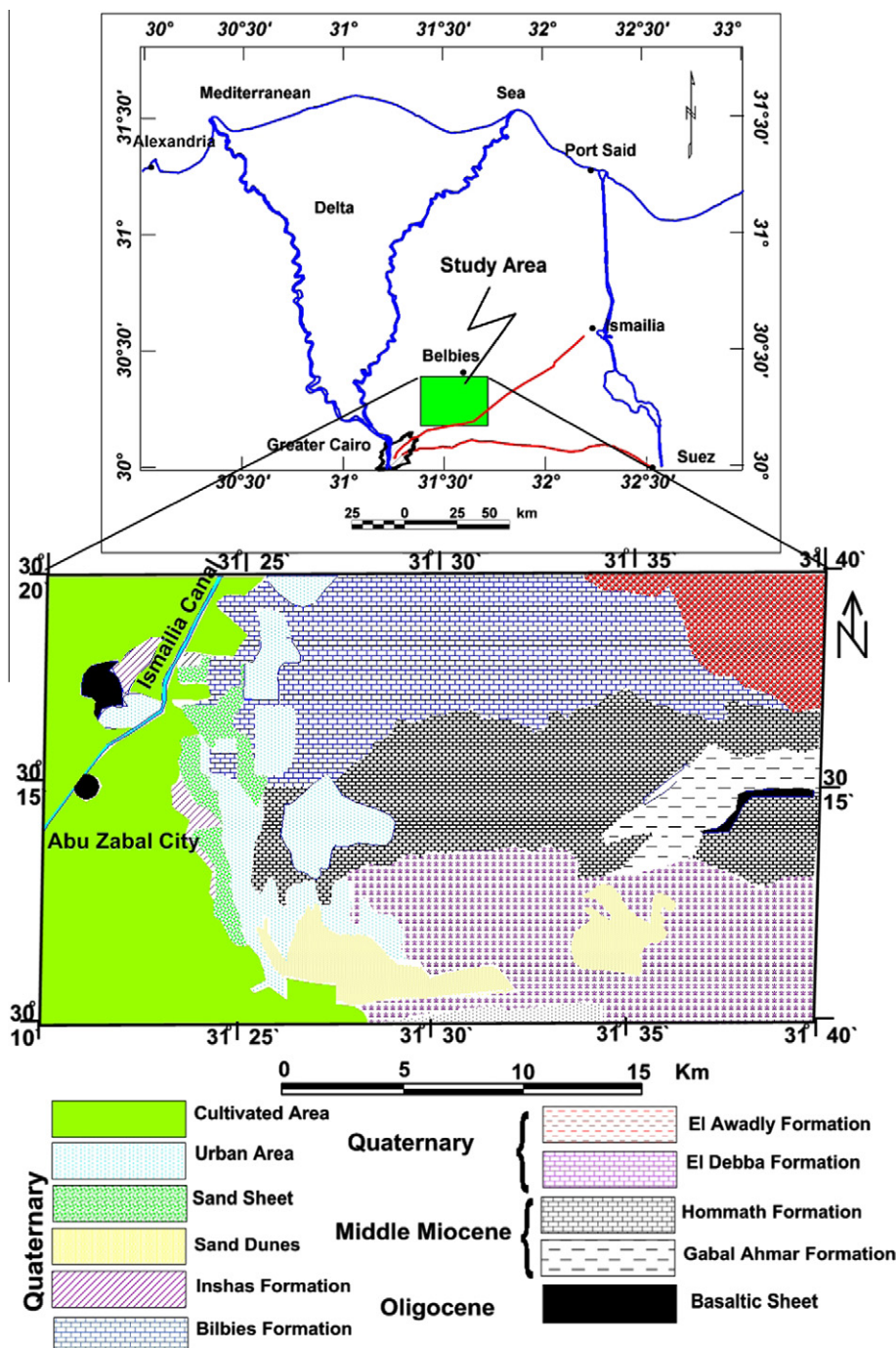

Fig. 1 (a) Location map of the surveyed zone, (b) geologic map of the study area.

Egypt falls along three major trends. The first major trend extends from the northern Red Sea area and along the Gulf of Suez, through the cities of Cairo and Alexandria. The second trend extends from the eastern Mediterranean to Cairo and Fayum region. The moderate earthquake of October 12, 1992 (Mb = 5.9) occurred on the intersection between the first trend and the second one near Cairo city. Along the third trend (Dead Sea-Aqaba trend), the seismic activity is large (Kebeasy, 1990). This may be related to the active sinistral movement along the Dead Sea Fault system and the Gulf of Aqaba (Reilinger et al., 1997; Elsayed et al., 2010). The present study aims to delineate structural fault elements specially the active fault elements and estimating depth of basaltic sheet which were related to the distribution of fault elements. The study area in this article is located at the northeastern part of Cairo, Egypt and bounded between latitudes 30°10′ & 30°20′N and longitudes 31°20′ & 31°40′ E covering an area of 661 km² (Fig. 1a).

Geological setting of the area

The geological setting of the study area has been constructed from the geological map published in 1998 by the Geological Survey of Egypt (Fig. 1b). The most part of the geological units in the study area are constituted by Quaternary, Middle Miocene and Oligocene deposits. The Quaternary deposits are represented by different formations such as sand sheets located at the eastern part of the area, sand dunes located at the central and southern part of the area. Inshas Formation is occupying the eastern part of the study area which consists of cross-bedded sand, intercalated with Nile mud and silt. Bilbies Formation is located at the northern part of the area and is made up of medium to coarse grained and cross-bedded sands with plant roots and carbonate pockets. El Awadly Formation covers the northeastern part and is mainly composed of cross-bedded gritty sands with plant roots. El Debba Formation, in the southeastern part of the area, consists of coarse grained sands intercalated with flint. The Middle Miocene is represented by Hommath Formation, which is located at the central part of the survey area and made up of interbedded yellow sandy limestone, sandstone and sandy marl. The Oligocene deposits are represented by Gabal Ahmar Formation and basaltic sheet. The Gabal Al Ahmar Formation is occupying the eastern part of the study area and is composed of sand and sandstone. Basaltic sheet is located at the northwestern part of the study area and lies at the north of Abu Zabal city. The geomorphology of the study area refers that the central part is characterized by high topography with the elevation gently decreasing toward north, west and south (Fig. 2)

Methodology

Magnetic data and interpretation

Land magnetic survey is carried out using two Envimag proton magnetometers with accuracy of 1 nT: one is used to record the magnetic field at one place (a base station lies in central part of the study area) in order to correct for diurnal variations of the magnetic field, while the second instrument is used for field measurements. Two thousand and two hundred stations are measured to cover the study area (Fig. 3a); the measured data is corrected for diurnal variation and for the effect of latitude. As the Earth's magnetic field strength varies from 25,000 nT at the magnetic equator to 69,000 nT at the poles, the increase in magnitude with latitude needs to be taken into account. Data acquired at any given location is subtracted from the normal field value obtained from the International Geomagnetic Reference Field (IGRF) (Reynolds, 1997). The values of IGRF are calculated at every field station then the values of diurnal variations and IGRF are subtracted. The corrected magnetic values are represented on a total intensity magnetic map (Fig 3b) with contour intervals of 10 nT using the Geosoft Program Oasis Montaj (2007).

It can be seen that there are high magnetic anomalies in the northwestern and northern parts of the area while the eastern and southern parts show low magnetic anomalies. The magnetic anomalies are due to shallow sources (basaltic sheet)
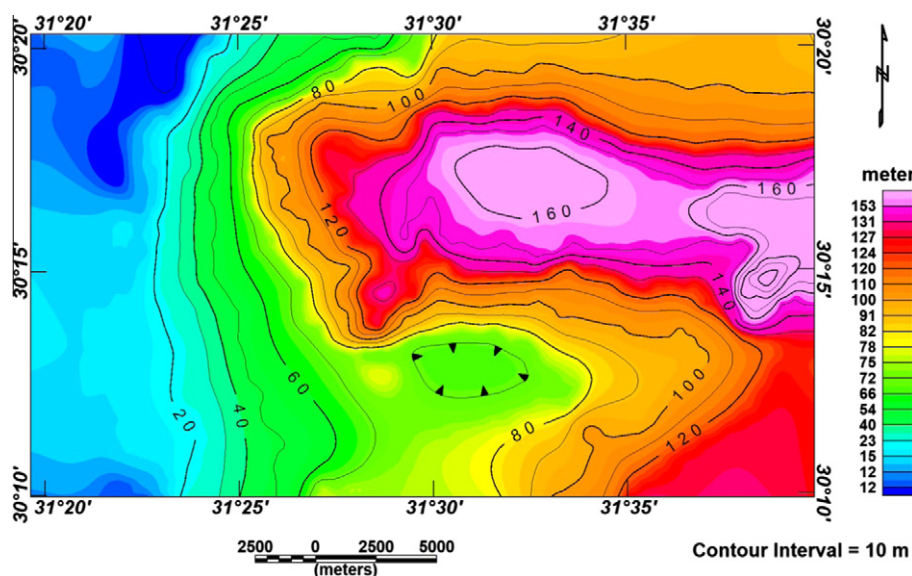

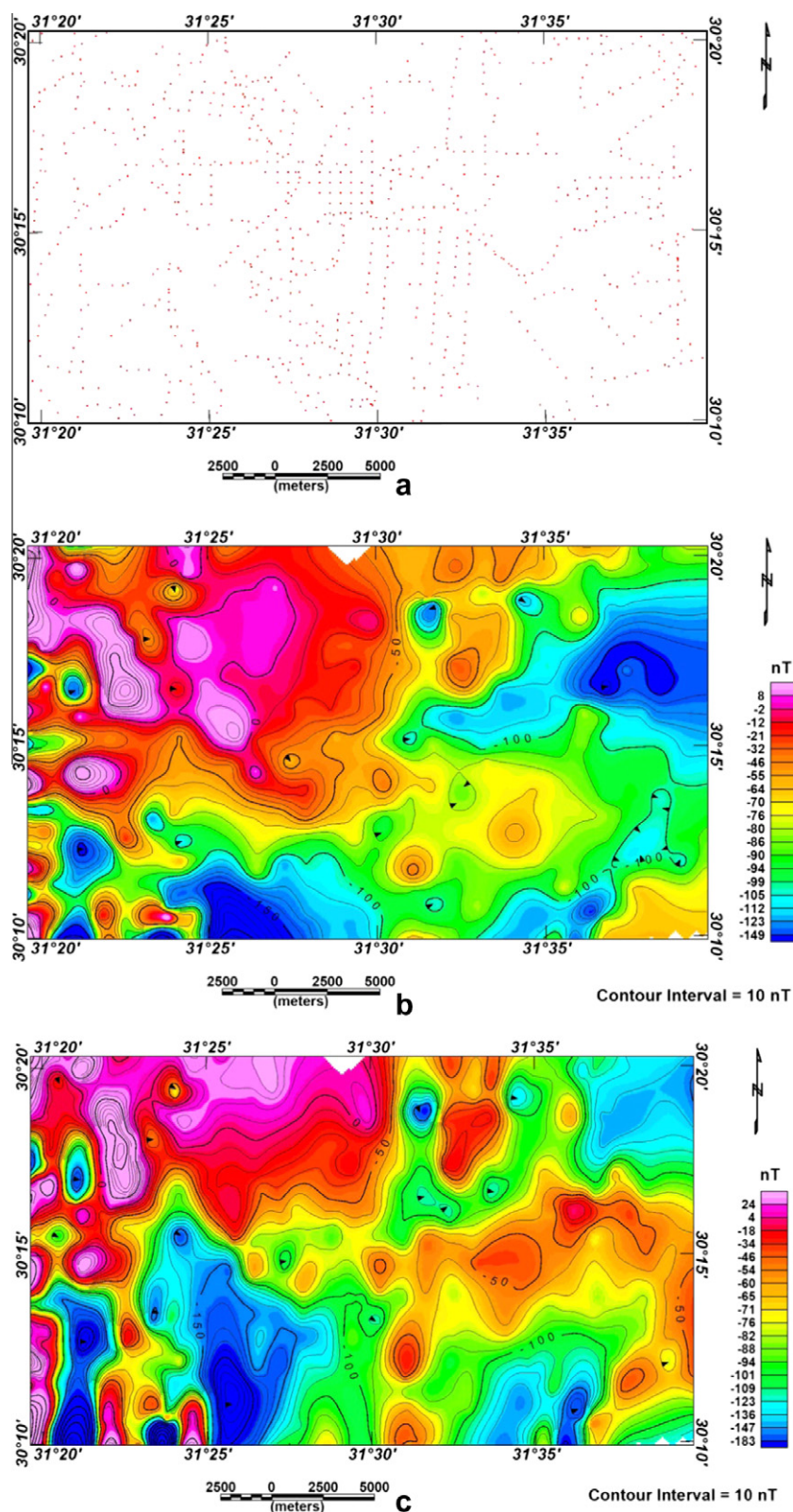**Fig. 2** Topographic map of the study area.

Fig. 3 (a) Locations of magnetic stations, (b) total intensity magnetic map, (c) the reduced to the pole (RTP) total intensity map.

and deep sources (basement rocks): the basaltic sheet is exposed at the surface in the western and eastern parts of the study area as shown in Fig. 1b. The magnetic fields due to geological bodies are distorted by the local inclination and declination of the magnetic earth's field, making difficult to estimate their shapes and locations correctly. In order to
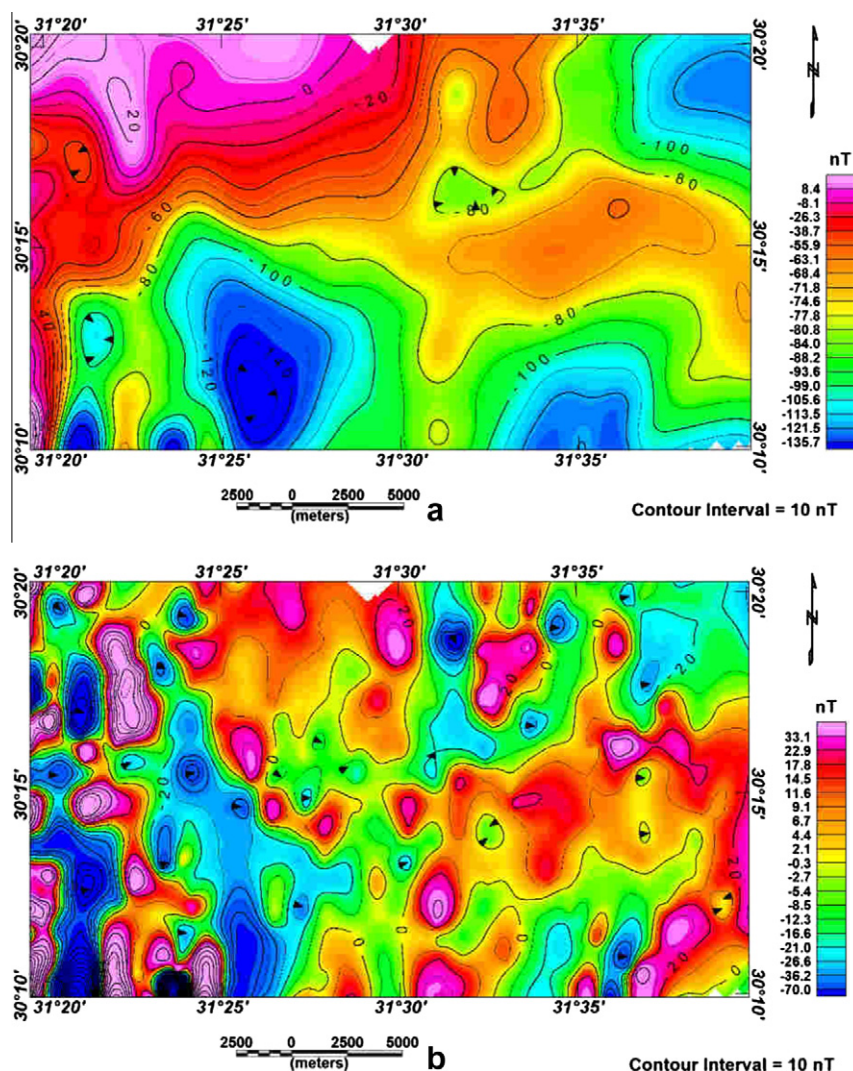
Fig. 4 (a) Upward continuation to an elevation of 1000 m, (b) residual map of basaltic sheet response.

eliminate that effect in the appearance of an anomaly, which depends on the magnetic latitude of the survey area as well as on the dip angle of the magnetization vector in the body, a mathematical procedure known by reduction to the pole (RTP) is applied to the grid of total magnetic intensity values using geosoft program (Oasis Montaj, 2007). The resultant map is then the reduced to the pole map (Fig. 3c), which is more usable, because its anomalies are independent on the magnetic inclination of the source bodies. The reduction to the pole procedure was first described by Baranov (1957), Baranov and Naudy (1964), Battacharyya (1965, 1967) and Baranov (1975). The field parameters used in this study to reduce the data to the pole are: magnetic inclination 44.03°, magnetic declination 2.6° and total field strength 43,007 nT.

The upward continuation technique is applied to the RTP total intensity map (Fig. 3c) to filter shallow sources (basaltic sheet) from the deep sources (basement complex). The upward continuation is carried out to an elevation of 1000 m where the magnetic signal of the basaltic sheet is expected to be null. In fact the depths of basaltic sheet are expected to ranges from zero (outcropping at the surface) to a maximum of 1 km. The Geosoft Programs (Oasis montaj), 2007 were used to

calculate the upward continuation map (Fig. 4a). This map is then subtracted from the RTP map (Fig. 3c) in order to produce the map of shallow sources illustrated in Fig. 4b.

Depth of basaltic sheet
The depth of the basaltic sheet that represents the shallow source of anomalies is estimated by using two techniques. The first is the Euler deconvolution and the other is 3-D magnetic modeling using GMsys-3D program (Geosoft Program-Oasis montaj, 2007). The Euler deconvolution technique is based on the Euler's homogeneity equation.

This homogeneity equation relates the magnetic field and its gradient components to the location of the source, with the degree of homogeneity N, which may be interpreted as a structural index (Thompson, 1982). The structural index is a measure of the rate of change of the field with distance. For example, the magnetic field of a narrow 2-D dyke has a structural index of $N = 1$, while a vertical pipe (or cylinder) have $N = 2$. The magnetic field originated by a step and contact have $N = 0$. In the present study, the depth of the magnetic sources is estimated through the application of the Euler deconvolution to the survey area using a window size of 10
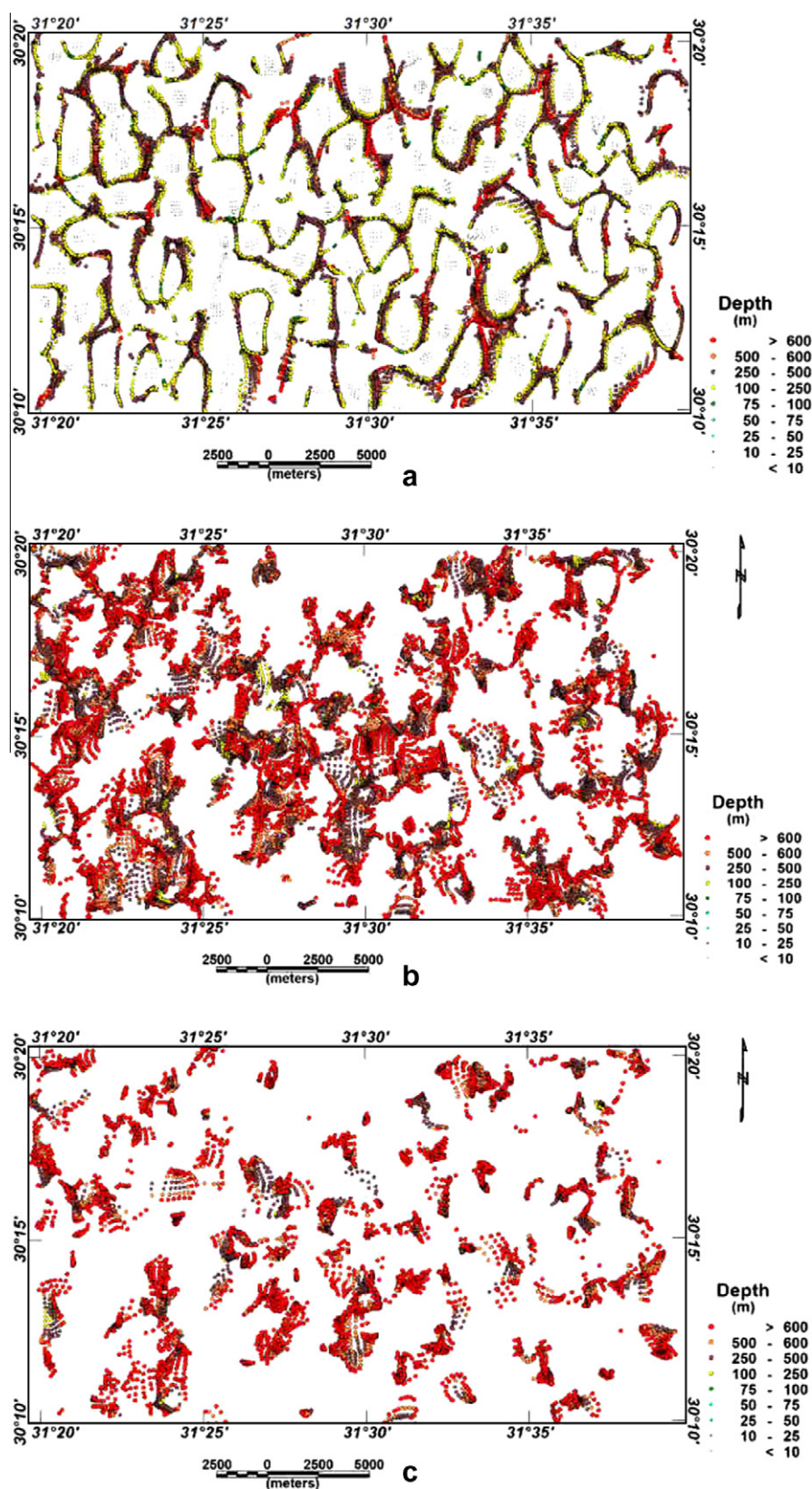
Fig. 5 Euler solution results, (a) structural index = 0, (b) structural index = 1, structural index = 2.

and various structural indices of 0, 1 and 2 in order to select the best structural index. The Euler solutions are presented

in Fig. 5a–c giving a picture of the distribution of the magnetic sources and their depths. The suitable structural index seems to
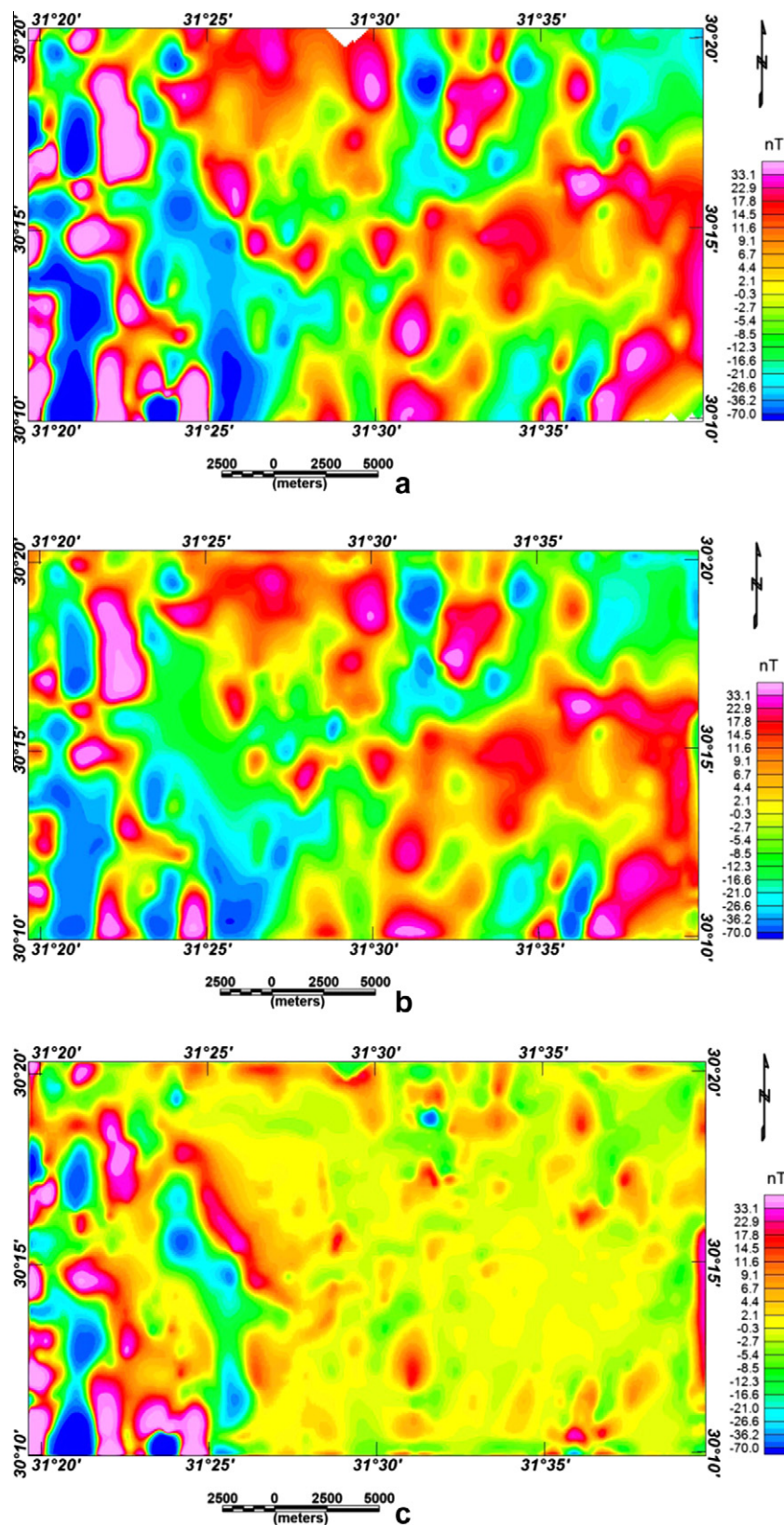
Fig. 6 outputs of GMSYS-3D modeling, (a) observed anomalies, (b) calculated anomalies and (c) deviation between calculated and measured anomalies (error).

be 0 (step and contact) which gives the tightest clustering of solutions as represented in the Fig. 5b.

The second technique to estimate the depth of basalt is the 3-D modeling. We have used the GMSYS-3D software, which
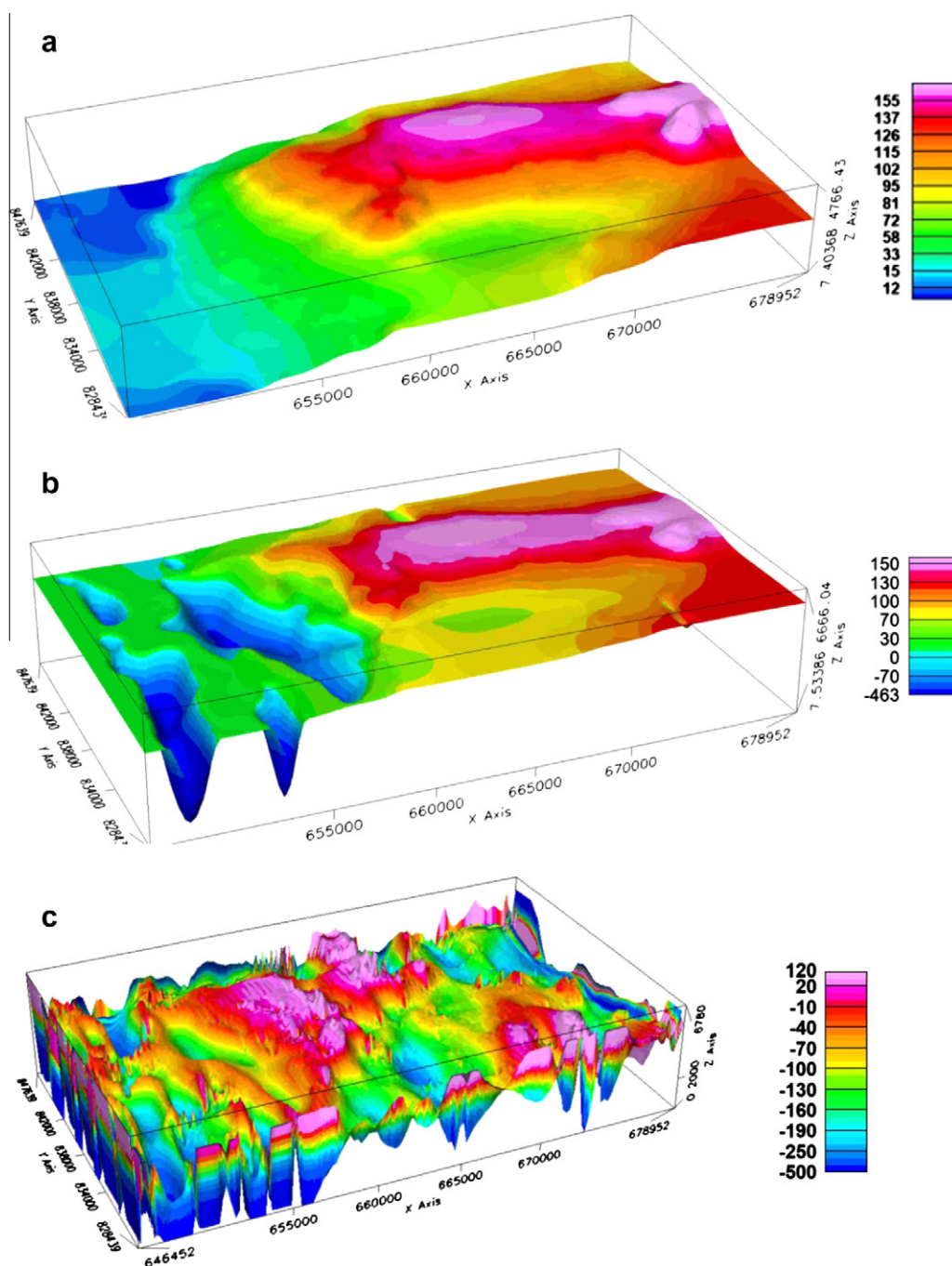
Fig. 7   Results of GMSYS-3D programs, (a) topography, (b) elevation of upper surface of basalt, (c) elevation of lower surface of basalt.

is one programs of the geosoft (Oasis Montaj, 2007). GMSYS-3D is a 3D gravity and magnetic modeling package for surface-oriented models. A model is defined by a number of stacked surface grids with density, susceptibility, and remnant magnetization-distributions specified for the layer below each surface (Figs. 6 and 7).

Gravity data and interpretation

Two thousand and two hundred stations are carried out at the same sites of magnetic measurements using an automatic gravity meter made by Scintrex (CG-3 Autograv) with resolution of

0.01 mGal (Fig. 8a). Different reductions are applied to gravity data, including drift, tide, latitude, free-air and Bouguer corrections. The corrected gravity data is then used to construct a Bouguer anomaly map (Fig. 8b) using Geosoftw program (Oasis Montaj, 2007). The gravity anomalies observed in the Bouguer field are caused by lateral density contrasts within the sedimentary section, crust and sub-crust of the earth.

Regional/residual separation of gravity data

The regional–residual separation technique is carried out to filter the regional component, which originates due to deep-seated sources from the residual component, which is related
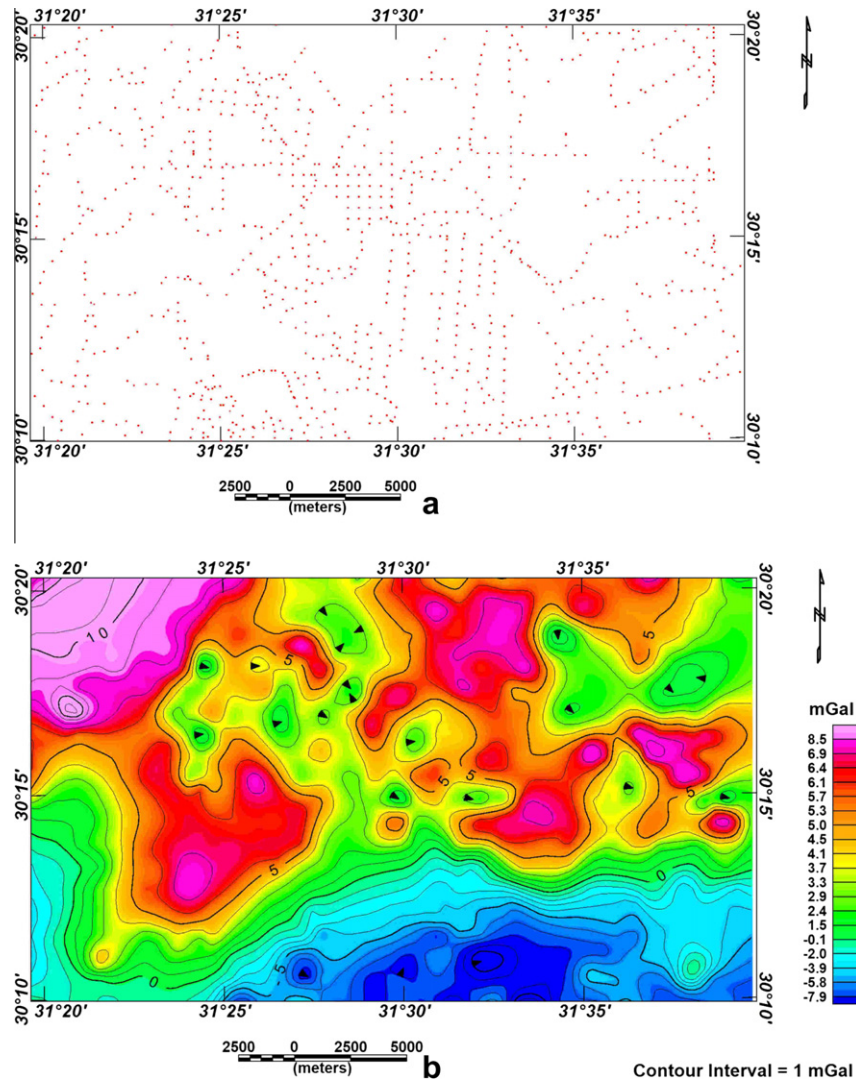
Fig. 8 (a) Location map of measured gravity stations; (b) Bouguer anomaly map.

to local, shallow structures. In the present study, we use the least squares technique to perform the gravity field separation. Calculations for different order up to fifth order have been used to estimate the best order of separation.

The results of the regional–residual separation for different orders have been mapped by Geosoftw Program (Oasis Montaj, 2007). Fig. 9(a–e), shows the regional component for first, second, third, fourth and fifth order, respectively.

Fig. 10(a–e), shows the residual component for first, second, third, fourth and fifth order, respectively. A correlation factor $r(x, y)$ has been calculated to select the best order of residual for gravity interpretation. The correlation factor can be estimated for any two orders such as correlation factor between i- and j- order for residual (rij), as in the following equation

$$rij(x, y) = \frac{\sum xy - \frac{(\sum x)(\sum y)}{2}}{\sqrt{\left[\left(\sum x^2 - \frac{(\sum x^2)}{n_x}\right)\left(\sum y^2 - \frac{(\sum y^2)}{n_y}\right)\right]}}$$

the correlation factor was calculated for the every two successive orders such as the correlation factor for first and second

order (r_{12}). Table 1 shows that the best order for gravity separation is the third order.

Seismicity of the study area

Long-term seismological records revealed that the source of seismicity of closest proximity to Cairo is the Eastern Mediterranean–Cairo–Fayoum trend, which is sometimes referred to as the Pelusiac trend. Kebeasy (1990) stated that this trend extends from the eastern Mediterranean to the east of the Nile Delta and through to Cairo and the Fayoum region. Along this trend, small to moderate earthquakes are observed, the depths of which are confined within the crust and do not define any seismic plane. The zone extends parallel to the Syrian Arc system, and hence Maamoun and Ibrahim (1978) attributed this low seismicity to the new-tectonic activity of the old dislocation zone (Syrian Arc system). Many of the events belonging to this trend occur in the Fayoum area southwest of Cairo such as the well-known Dahshour earthquake of 12 October 1992, a fact that encouraged some researchers to consider Fayoum area as a separate seismic zone (Abu El-Enein, 1997).
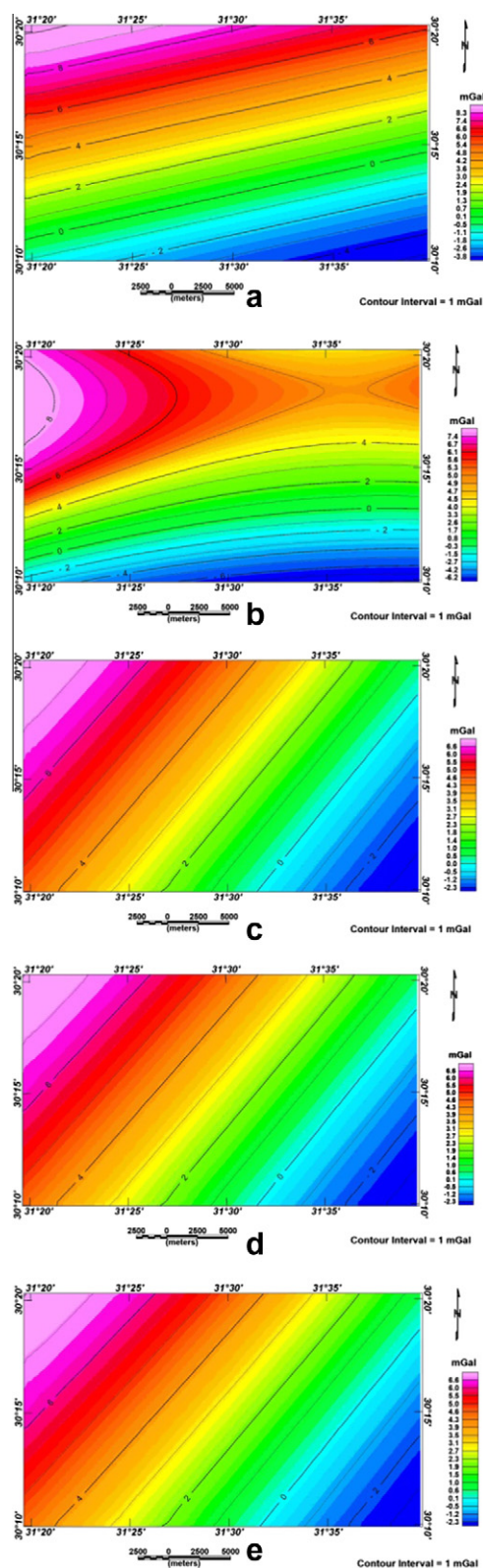
Fig. 9 Regional maps for (a) first order, (b) second order, (c) third order, (d) fourth order and (e) fifth order.

Fig. 10 Residual maps for (a) first order, (b) second order, (c) third order, (d) fourth order and (e) fifth order.

A recent study by Moharram et al. (2008) demonstrated that the seismicity in the region is mainly associated with six tecton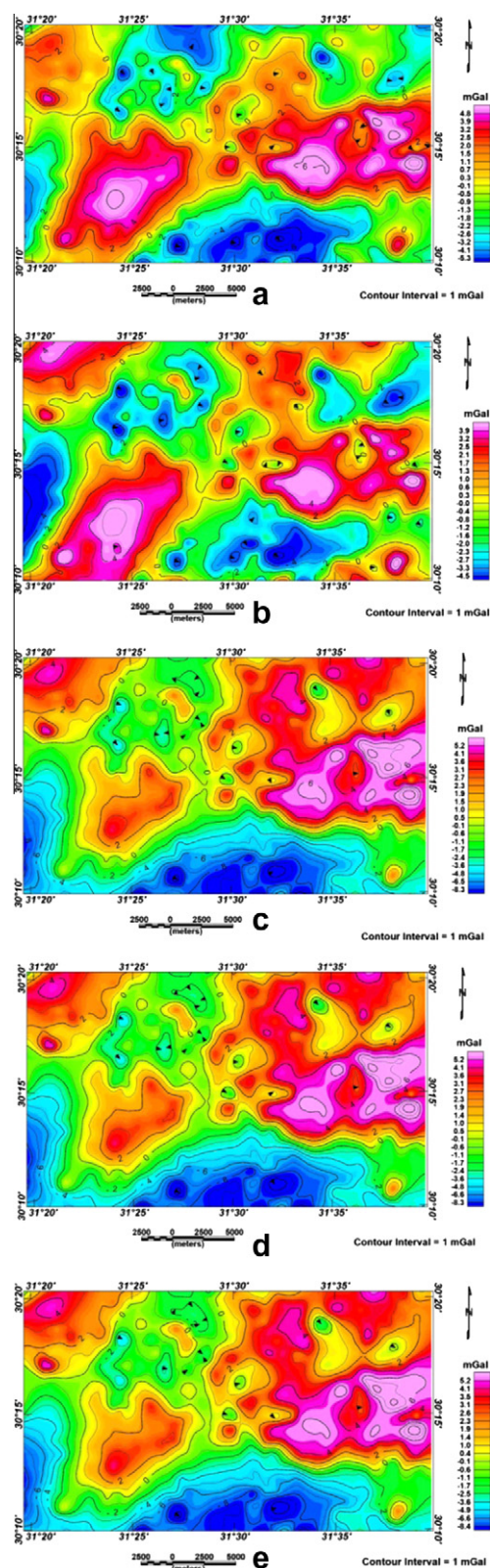ic trends, namely the Levant–Aqaba transform system, the northern Red Sea–Gulf of Suez–Cairo–Alexandria trend (Suez trend), the Eastern Mediterranean–Cairo–Fayoum trend, Hellenic and Cyprian arcs, Mediterranean coastal
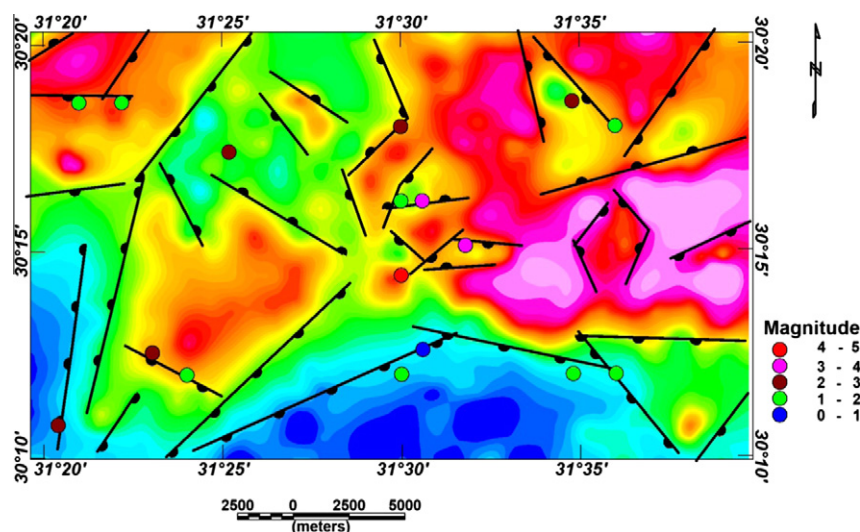
Fig. 11 Location of possible faults as inferred from the residual gravity map of the study area combined with the earthquake events compiled in the study area.

Table 1 Correlation factor for different orders.

Order	Value
r_{12}	0.919825
r_{23}	0.666593
r_{34}	0.999966
R_{45}	0.999966

dislocation, and the southern Egyptian trends. Accordingly, Greater Cairo is remote from any major plate boundaries, with the closest major source being the Suez Rift. The Suez rift forms part of the Suez trend, dominated by normal faults striking parallel to the rift's axis.

Twenty-four events in the study area were recorded and analyzed by the National Research Institute of Astronomy and Geophysics (NRIAG).

Results

The results of magnetic interpretation through using Euler solutions indicate that the depth of basalt is ranging from outcrop to 600 m. The results of 3-D magnetic modeling shows good compatible between observed and calculated magnetic data (Fig. 6). Also, the results of the 3-D magnetic modeling reveal the elevations of different surface (Fig. 7): the topography surface in Fig. 7(a), which ranges from 12 to 155 m above sea level, the elevation of upper surface of basalt (Fig. 7b), ranging from −463 to 150 m above sea level and the elevation of lower surface of basalt (Fig. 7c) ranging from −500 to 120 m above sea level.

The third order residual gravity map has been used for gravity interpretation to delineate the structural elements that dissect study area. The fault map (Fig. 11) shows different fault elements of different direction such as NW–SE trend parallel to the Gulf of Suez trend, the NE–SW one, which is parallel to Gulf of Aqaba and the E–W trend parallel to the trend of Mediterranean Sea.

The magnitudes of the recorded seismic events range from 1 to 4.3 on Richter scale, while depths to their foci vary from 4 to

20 km. Most of the events are recent ones recorded from 1962 to 2003 and hence can be considered to indicate a neo-tectonic situation. The seismicity data are listed in Table 2 and illustrated in Fig. 11.

Discussion

The capital of Egypt, Greater Cairo is a subject of civil expansions and developments. A successful and efficient planning for such developments is in need for an overview on the geological structural elements that may affect any urban or civil constructions. Detailed magnetic and gravity surveys are carried out around Greater Cairo in Egypt with the aim to deduce the main structural elements that exist in this region. More than 2000 magnetic points and more than 2000 gravity stations could be measured in a fairly homogeneous distribution around the city. After correction and reduction of both data sets a reduced to the pole (RTP) magnetic anomaly map and a Bouguer gravity map are constructed.

In order to extract the anomalies due to shallow objects, regional separation procedures have been applied to both maps. Upward continuation and the least squares method are found to be efficient techniques in regional calculations of magnetic and gravity surveys respectively. Euler deconvolution is applied to the shallow RTP magnetic anomalies to locate the fault elements. Furthermore a 3-D magnetic model is constructed for the basalt that is known to be the source of the anomalies. On the other hand the residual Bouguer anomaly map is used to locate the qualitatively expected faults in the region. Finally, a record of 24 recent seismological events are considered to evaluate the activity of the faults deduced from both magnetic and gravity measurements.

The main result of the work is that the study area is dissected by different active faults. These faults are affecting the distribution and configuration of the basaltic sheet, which is the main element of the subsurface in the region. The 3-D modeling of the magnetic data reveals that the depth of this basaltic sheet is varying according to the structural elements. The interpretation of the gravity data confirms the result, that the study area is dissected by different fault systems. The seismological records

Table 2 List of earthquake events recorded during the period from 1900 to 2005 in and around the study area.

Event No	Longitude	Latitude	Year	Depth	Magnitude
1	31.34	30.18	2003	12	2.2
2	31.4	30.2	1968	20	1.9
3	31.4	30.2	1970	20	1.4
4	31.5	30.2	1976	20	2.2
5	31.5	30.2	1967	20	2.5
6	31.5	30.2	1976	20	1.8
7	31.58	30.2	2000	28	2
8	31.6	30.2	1978	20	1.9
9	31.384	30.209	1992	4	2.3
10	31.51	30.21	2003	14	1
11	31.51	30.21	2003	14	1
12	31.5	30.24	1999	14	4.3
13	31.53	30.252	1992	14	3.1
14	31.5	30.27	1997	18	1.3
15	31.51	30.27	1999	14	3.2
16	31.42	30.29	1999	20	2.8
17	31.5	30.3	1962	20	1
18	31.5	30.3	1987	25	2.5
19	31.6	30.3	1978	20	2.1
20	31.6	30.3	1976	20	1.5
21	31.35	30.31	2000	20	1.6
22	31.37	30.31	2003	6	2
23	31.58	30.31	2001	20	2.2
24	31.34	30.18	2003	12	2.2

indicate that the faults are active. Some of the faults are known to be active and already as they caused some damage for buildings and constructions at the western part of the study area. More over groundwater at the central part of the region moved up along an active fault due to the earthquake event number 12 of magnitude 4.3 (Table 2) so that a lake of water was accumulated near the urban area of dense population. Most of seismic events which recorded in the study area are distributed along the fault elements which are delineated from gravity interpretation; also the magnetic interpretation indicates that the western and northern parts exhibit shallow depths of the basaltic sheet. These shallow depths of basaltic sheet reflect that these parts are affected by these fault elements.

Conclusion

From the quantitative interpretation of the magnetic, gravity and seismological data, we can conclude that:

1. The fault elements dissecting the area are active and have characteristic trends of NW–SE, NE–SW and E–W.
2. Depth of the basaltic sheet ranges from less than 10–600 m.
3. The recent records of seismological events in the period from 1992 to 2003 include magnitudes in the range of 1–4.3 on Richter scale.
4. The central and western parts are characterized by seismological activity due the active fault elements.
5. The detailed geophysical investigation must carried out before any construction planning.

References

Abu El-Enein, K.A., 1997. Study on the seismotectonics of Egypt in relation to the Mediterranean and Red Sea tectonics. Ph.D. thesis, Ain Shams University, Cairo, Egypt.

Abou Elenean, K.M., Mohamed, M.E., Hussein, H.M., 2009. Source parameters and ground motion of the Suez–Cairo shear zone earthquakes, Eastern Desert, Egypt. Nat. Hazards. http://dx.doi.org/10.1007/s11069-009-9388-x.

Baranov, V., 1957. A new method for interpretation of aeromagnetic maps: pseudo-gravimetric anomalies. Geophysics 22, 359–383.

Baranov, V., Naudy, H., 1964. Numerical calculation of the formula of reduction to the magnetic pole. Geophysics 29, 67–79.

Baranov, V., 1975. Potential fields and their transformation in applied geophysics. Geoexploration Monographs, series 1–6. Gebrüder Borntraeger, Berlin, Stuttgart.

Bhattacharyya, B.K., 1965. Two dimensional harmonic analysis as a tool for magnetic interpretation. Geophysics 30 (5), 829–857.

Bhattacharyya, B.K., 1967. Some general properties of potential field in space and frequency domains: a review. Geoexploration 5, 127–143.

Issawy, E.A., Radwan, A.H., Ddhy, S.A., Rayan, A., 2010. Monitoring of recent crustal movements around Cairo by repeated gravity and geodetic observations. Contrib. Geophys. Geodesy J. 40 (2), 173–184.

Geological Survey of Egypt (EGSMA), 1998. Geology of Inshas Area, Geol. Surv. Egypt, internal report.

Geosoftw Program (Oasis Montaj), 2007. Geosoft mapping and application system, Inc., Suit 500, Richmond St. West Toronto, ON, Canada N5SIV6.

Kebeasy, R.M., 1990. Seismicity. In: Baklema. (Ed.), Geology of Egypt. Rotterdam, pp. 51–59.

Maamoun, M., Ibrahim, E., 1978. Tectonic activity in Egypt as indicated by earthquakes. Helwan Inst. Astronom. Geophys. Bull. 170.

Moharram, A.M., Elghazouli, A.Y., Bommer, J.J., 2008. A framework for a seismic risk model for Greater Cairo. Soil Dynam. Earthquake Eng. 28, 795–811.

Monteiro Santos, F.A., Sultan, S.A., 2008. On the 3-D inversion of vertical electrical soundings: application to the South Ismailia Cairo Desert Road area, Cairo, Egypt. J. Appl. Geophys. 65, 97–110.

Reilinger, R.E., McClusky, S.C., Oral, M.B., King, R.W., Toksoz, M.N., 1997. Global Positioning System measurements of present-day crustal movements in the Arabia-Africa-Eurasia plate collision zone. J. Geophys. Res. 102 (B5), 9983–9999.

Reynolds, J.M., 1997. An Introduction to Applied and Environmental Geophysics. Wiley, Chichester, pp. 796.

Sultan Araffa, Sultan Awad, 2010. Geophysical investigation for shallow subsurface geotechnical problems of Mokattam area, Cairo, Egypt. Environ. Earth Sci. J. 59, 1195–2207.

Sultan, S.A., Santos, F.A.M., 2008. Evaluate subsurface structures and stratigraphic units using 2-D electrical and magnetic data at the area north Greater Cairo, Egypt. Int. J. Appl. Earth Observ. Geoinf. 10, 56–67.

Sultan, Sultan Awad, Monteiro Santos, Fernando A., Abbas, Abbas Mohamed, 2010. Joint Inversion interpretation for gravity and resistivity data: case study at New Helioplis City, Cairo, Egypt. Near Surf. Geophys. J. 8, 43–53.

Thompson, D.T.T., 1982. Euler, a new technique for making computer assisted depth estimates from magnetic data. Geophysics V. 47, 31–37.